



Radical Decomposition of Ether-Based Electrolytes for Li-S Batteries

Lucas Lodovico,^{a,b} Alberto Varzi,^{a,b,z} and Stefano Passerini^{a,b,*,z}

^aHelmholtz Institute Ulm (HIU), 89081 Ulm, Germany

^bKarlsruhe Institute of Technology (KIT), 76021 Karlsruhe, Germany

In this work, the stability of ether-based electrolytes for Li-S batteries is investigated with particular regard to the effect of dissolved oxygen. Specifically, the performance of two different electrolyte solvents, i.e., 1,2-dimethoxyethane and its mixture with 1,3-dioxolane (DME:DOL, 1:1 v/v), is characterized in cells assembled in dry air environment, which would substantially lower production costs with respect to inert atmosphere (Ar). Although stability of all the components would suggest that Li-S batteries built in both the environments should behave similarly, it is found that cells containing the DME:DOL-based electrolyte are rather unstable in the presence of O₂ in contrast to those employing DME-based electrolyte, which show a relatively good performance. The different sensitivity toward O₂ of these electrolytes is associated to the ring-opening reaction of DOL, which happens to a greater extent when O₂ is present, but occurs also in its absence. Based on these results a mechanism for electrolyte degradation in Li-S cells, and its reaction with dissolved polysulfides is proposed, which rationally explain for the first time the behavior already reported in literature for these kind of batteries. These findings are also relevant to the field of Li-O₂ batteries, where these ether-based electrolytes are also used.

© The Author(s) 2017. Published by ECS. This is an open access article distributed under the terms of the Creative Commons Attribution 4.0 License (CC BY, <http://creativecommons.org/licenses/by/4.0/>), which permits unrestricted reuse of the work in any medium, provided the original work is properly cited. [DOI: 10.1149/2.0311709jes] All rights reserved.



Manuscript submitted April 14, 2017; revised manuscript received May 24, 2017. Published June 21, 2017.

Sulfur has been extensively investigated as a new cathode material for secondary batteries, in order to replace metal oxides normally used in lithium-ion batteries (LIBs). The first point of interest is its high theoretical specific capacity, around 1672 mAh g⁻¹, but, as a raw material sulfur is also non-toxic, readily available, and very inexpensive. It is indeed one of the main side products of crude oil refining, with more than 60 million tons produced annually.¹ Even the relatively low operating voltage of sulfur-based cathodes, at around 2 V vs. Li/Li⁺, can be considered as a potential advantage, making it intrinsically safer.² Furthermore, the high specific gravimetric capacity of sulfur enables the remarkable specific energy of about 2600 W h kg⁻¹. However, Lithium-Sulfur batteries (LSB) still present some specific challenges that need to be solved to enable their commercialization.² First, sulfur has a very low electrical conductivity, around 5 × 10⁻³⁰ S cm⁻¹ at 25°C, requiring the introduction of a conductive matrix, normally carbon-based. The carbon host is generally electrochemically inert, such that it decreases the energy density of the electrode as whole, especially since it is often near to 50 wt% of the total sulfur-composite mass. Secondly, and most importantly, sulfur is a conversion material undergoing several chemical transformations during discharge and forming a variety of different polysulfides with the formal oxidation state of sulfur changing from 0 to -2. Some of these intermediate species are soluble in the electrolyte, and very reactive toward both the electrolyte itself^{3,4} and the lithium metal anode.^{2,5} Most importantly though, their dissolution causes the loss of active material and, during charge, the so-called shuttle mechanism, i.e., the transfer of electrons from the negative to the positive electrodes.^{6,7} Finally, in the fully reduced state, Li₂S has low electrical and ionic conductivities, and is even less dense than sulfur. The poor conductivities result in the sulfide to be hardly re-oxidized, which leads to cell irreversibility and, in turn, capacity loss. The lower density means that, upon full reduction, the cathode volume increases, thus the sulfur electrode (i.e., the cell) must be capable of accommodating the volume expansion.

State-of-the-art LSBs' electrolytes are constituted by ether solvents, or a mixture thereof,³ a lithium salt, and, optionally, an additive.⁸⁻¹⁰ The choice of ethers as solvent comes from their stability toward polysulfides. The superior chemical stability of ethers was also shown to be relevant for Li-O₂ batteries, for instance.¹¹ Similarly to LSBs, Li-O₂ batteries rely on a conversion cathode (i.e., oxygen), which forms highly reactive intermediates that readily react with conventional carbonate-based electrolytes, leading to their

decomposition. This problem appears to be relieved in ether-based electrolytes.

Taking this in consideration, the electrochemistry of Li-S cells in a dry air environment is herein assessed. Building cells in dry air, in fact, could substantially lower production costs when compared to assembly in inert atmosphere (Ar). Although the stability of all the components would suggest that they should behave similarly in both cases, the effect of dissolved oxygen from dry air in the state-of-the-art electrolyte for LSBs (consisting of 1 mol L⁻¹ LiTFSI and 0.25 mol L⁻¹ LiNO₃ in a mixture of 1,2-dimethoxyethane and 1,3-dioxolane (DME:DOL, 1:1 v/v)) and its role on the electrochemical stability of the battery, necessitate a deeper investigation. For comparative purposes, cells were also assembled using a similar electrolyte, containing only DME as solvent. Electrochemical and *post mortem* analysis allowed to develop a more detailed model of the chemical and electrochemical reactions that take place inside a LSB, as well as to determine which classes of solvents are less sensitive to the presence of air and could, therefore, enable the electrolyte filling step to be performed in non-inert (but still dry) environment.

Methods

Preparation of electrolytes.—Two sets of electrolytes were prepared and tested, one under dry air and one under argon (Figure S2). Electrolytes were prepared using 1,2-Dimethoxyethane (DME, Solvionic) and 1,3-Dioxolane (DOL, Solvionic) as solvents. Each solvent was dried using 20 wt% molecular sieve (3Å, Alfa-Aesar) for 24 h. The water content was reduced below 10 ppm as determined by coulometric Karl Fischer titration (Mettler-Toledo Titrator Compact C30). For the DME:DOL-based electrolyte stored in dry air, the dried solvents were mixed in a 1:1 volumetric ratio, and the appropriate amount of lithium bis(trifluoromethanesulfonyl)imide (LiTFSI, battery grade 3 M) and lithium nitrate (LiNO₃, Alfa Aesar) were added, in order to achieve 1 mol L⁻¹ and 0.25 mol L⁻¹ concentrations, respectively. Dry DME was also used as the only solvent to prepare the electrolyte with the same LiTFSI and LiNO₃ concentrations. The two electrolytes prepared and stored under dry air are hereinafter labeled as DME:DOL air and DME air. The same electrolytes compositions without exposition to air were also prepared as it follows. The dried solvents were degassed, each individually, via the Freeze-Pump-Thaw method. Briefly, each solvent was frozen in liquid nitrogen (LN₂) and then subjected to vacuum until a final pressure of less than 10⁻³ mbar was achieved. The flask containing the solvent was then disconnected from the vacuum pump and allowed to melt under static vacuum.

*Electrochemical Society Member.

^zE-mail: alberto.varzi@kit.edu; stefano.passerini@kit.edu

This step was repeated three times for each solvent. Afterwards, the solvents were transferred and stored in an Ar-filled glove-box (MBraun) with O₂ and H₂O content lower than 0.1 ppm. Dried and degassed DME and DOL were used to prepare the electrolyte solutions with the above-mentioned compositions. These electrolytes, prepared and stored under Ar, are labeled hereinafter as DME:DOL Ar and DME Ar.

Preparation of the sulfur cathode.—Sulfur composite cathodes (AC/S) were prepared by impregnation of sulfur in an activated carbon matrix. Specifically, 1 g of sulfur (Sigma-Aldrich) was dissolved in 65 mL of cyclohexane (Sigma Aldrich) at 70°C and added to 0.2 g of activated carbon (DLC Super30, Norit). The resulting slurry was sonicated for 40 minutes and further stirred for one hour at 60°C, and for 24 h at 30°C. The solid material was then filtered and dried at 50°C under vacuum to remove the solvent. The sulfur content was determined to be 52 wt% (Figure S1) by thermogravimetric analysis (TGA, Netsch) performed at a heating rate of 10°C min⁻¹ in N₂ atmosphere, from 80°C to 500°C. The weight percent of sulfur was calculated as the difference between the initial and the final mass of the composite, i.e., assuming that only but all sulfur sublimated by heating.

The AC/S composite was then mixed with polyvinylidene fluoride (PVdF 6020, Solvay) and SuperC65 (Imerys Graphite & Carbon), as binder and conductive carbon, respectively, in the ratio of 85:5:10. N-Methyl-2-pyrrolidone (NMP, Sigma Aldrich) was used as solvent to prepare the slurry. Electrodes were cast onto aluminum foils using the Doctor blade method. The electrode layer was firstly dried at 60°C under normal atmosphere to remove the solvent and then punched into 12 mm diameter discs. Finally, the electrode disks were further dried overnight at 50°C in vacuum to remove solvent and water traces before being used for the electrochemical characterization. The final sulfur mass loading of the electrodes was ~1 mg_s cm⁻².

Electrochemical characterization.—Three-electrode, Swagelok-type T-cells were assembled inside an Ar-filled glove box (O₂ and H₂O < 0.1 ppm), using AC/S composite disk as working electrode, 12-mm disk lithium metal (Albemar) as anode, and a lithium metal strip as reference electrode. Glass fiber discs (Whatman GF/A) were used as separator, soaked with ~100 μL of electrolyte. To prevent short-circuits, four layers of glass fiber were used between the counter and working electrodes. The reference electrode consisted of a thin strip of lithium attached to a Ni grid, with 2 mm length, inserted in-between the four separator layers.

Cells with electrolytes under Ar were assembled inside the glove box. The O₂ containing electrolytes were sealed inside a bubble-free blister, and brought inside the glove box. Once inside, the blister was punctured using a syringe needle, and the extracted electrolyte quickly added to the separator, and the cell sealed, to avoid gas exchange with the argon environment.

All galvanostatic measurements were performed at a constant rate of C/10 (1 C = 1675 mA g_s⁻¹) between 3.0 and 1.5 V vs Li/Li⁺ using a Modulab XM ECS (Solartron Analytical). After each cycle, the sulfur electrodes were held at 3.0 V for 20 minutes to ensure full delithiation of the cathode and bring the system to a stable condition (the current typically dropped below C/30) and analyzed by potentiostatic electrochemical impedance spectroscopy (EIS), from 250 kHz to 10 mHz, with a sinus amplitude of 5 mV. All tests were performed in a climatic chamber at 20°C (Binder). Each cell was run for a total of 10 discharge/charge cycles and, finally stopped in the charged state (3.0 V vs Li/Li⁺) for the *post mortem* analysis.

Post mortem analysis.—After cycling, all cells were disassembled inside an Ar-filled glove box. The sulfur cathodes were gently but carefully washed with DME to remove any salt residue, and stored under Ar. To recover the electrolyte, the separators were placed inside a sealed vial and centrifuged at 6000 rpm for 60 min.

The cathodes were subjected to scanning electron microscopy (SEM, Zeiss LEO 1550 VP), with an acceleration voltage of 3 kV. To

avoid any contamination by air, all samples were transferred inside the SEM chamber using a sealed sample carrier filled with Ar.

The cathodes were also analyzed by X-ray photoelectron spectroscopy (XPS, PHI 5800 MultiTechnique ESCA System, Physical Electronics), using a monochromatic Al-Kα (1486.6 eV) radiation. The measurements were performed with a detection angle of 45°, using pass energies at the analyzer of 93.9 and 29.35 eV for survey and detail spectra, respectively. The samples were transferred to the device using a sealed sample carrier to avoid air contamination. All XPS spectra were calibrated to the signal of the C(1s) peak at 284.6 eV and analyzed using CasaXPS software. For the analysis of the sulfur spectra, the S(2p_{1/2}) peaks were constrained to be shifted +1.16 eV with respect to the corresponding S(2p_{3/2}) peaks, while having 0.511 times their area, and the same full width at half maximum (FWHM).

Both the fresh electrolytes and those recovered from cycled cells were analyzed by infrared spectroscopy (IR, PerkinElmer) in the attenuated total reflectance (ATR) mode. All ATR-IR measurements were performed in dry argon atmosphere (glove box).

Results and Discussion

Figures 1a and 1c have very similar voltage profiles, in agreement with the typically poor cycling behavior of sulfur cathodes.¹² The discharge profile consists of a plateau at ca. 2.4 V, a sloping region from ca. 2.3 to 2.1 V, and another, longer, plateau at ca. 2.1 V. The high voltage plateau at 2.4 V is due to the reduction of S₈ to high order polysulfides (Li₂S₆₋₈). In the sloping region, these are reduced to form shorter polysulfides (Li₂S₄), which are further reduced at ca. 2.1 V to solid Li₂S₂ and Li₂S, i.e., the final discharge products. It is important to note, however, that many disproportionation reactions take place in such a system, and the exact nature of the formed species upon reduction is still not fully known.^{12,13} The abovementioned species represent what the average chain length is expected to be in each case. Finally, the last plateau at ca. 1.7 V is probably associated to the irreversible reduction of LiNO₃ on the positive electrode,¹⁴ which eventually vanishes due its complete consumption upon cycling.

Interestingly, the presence of air in the electrolyte appears to be less relevant for the electrolyte based on DME as the only solvent, as testified by the similar voltage profiles of the cells employing DME Ar and DME air (Figures 1a and 1b, respectively), although with a higher fading of the latter. A first feature to be noticed is the lack of any sign of oxygen reduction in the DME air electrolyte. Oxygen reduction should be expected at about 2.6–2.7 V vs Li/Li⁺,^{15,16} while in Figure 1b, no plateau at this potential is detected. This is, however, not surprising, since most of the O₂ is likely reacting with the lithium anode, as soon as the cell is assembled. The only indication of O₂ presence is the slightly higher open circuit potential (OCP) before the experiment started (ca. 3.3 V in air vs ca. 2.8 V in Ar), possibly due to the reaction of sulfur with oxygen, forming lower sulfur oxides. Such oxides might explain the higher OCP observed in this case.

A further substantial difference between DME Ar and DME air is the more pronounced capacity fading of the latter (see Figure 1e). A possible explanation would be the oxidative decomposition of DME, which can form, among other, inorganic carbonates and esters.¹⁷ Sulfides and polysulfides are known for their high nucleophilicity, in part due to the large atomic volume of sulfur, making them readily polarizable. Organic thiolates, which have a negatively charged sulfur atom analogous to sulfides and polysulfides, have been shown to be highly reactive toward organic esters,¹⁸ resulting in their cleavage. Therefore it is not unlikely that polysulfides formed during discharge of sulfur cathodes can also react with organic carbonates via nucleophilic attack,⁴ forming (poly)-thioesters. Hence, the carbonates and esters formed by oxidation of DME in presence of air are expected to react with dissolved polysulfides formed during discharge, decreasing the available amount of active material and, in turn, leading to a more pronounced capacity fade in each cycle, when compared to the air-free DME electrolyte.

DME:DOL air (see Figure 1d), on the other hand, shows a rather different behavior compared to the DME:DOL Ar. The first cycle

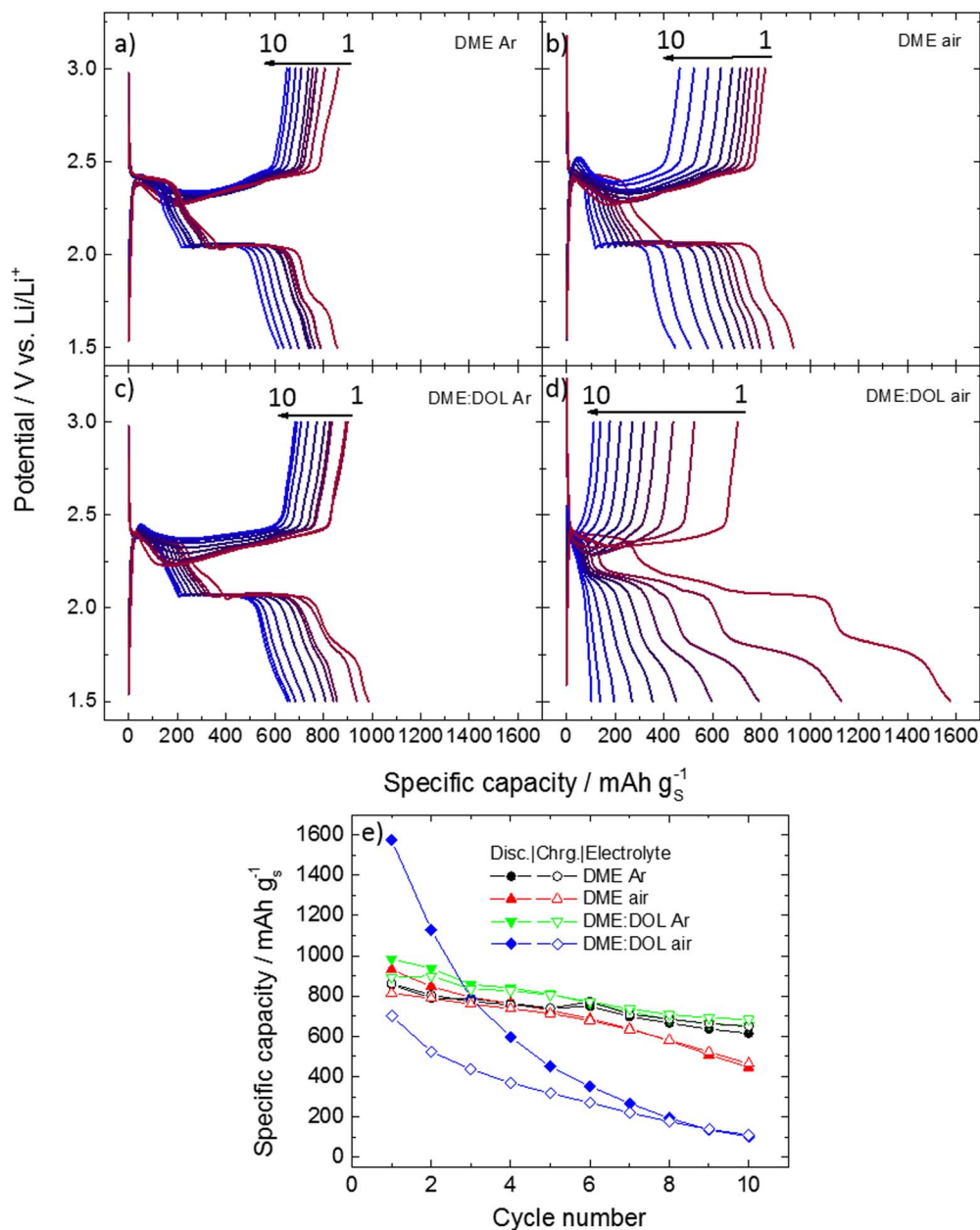


Figure 1. Voltage profiles of Li-S cells with different electrolytes: (a) DME Ar, (b) DME air, (c) DME:DOL Ar, and (d) DME:DOL air. (e) Capacity retention upon 10 cycles of the Li-S cells employing different electrolytes.

capacity is much larger (ca. 1600 mAh g_s⁻¹) than with any other electrolyte investigated herein. This is mainly due to the increased discharge capacity in the sloping region comprised between 2.25 and 2.08 V (see Figure S3), and to the higher charge arising from nitrate reduction, accounting for a respective increase of capacity, in these regions, of 178% and 116%, with respect to the other electrolytes. This higher discharge capacity of nitrate is likely associated to larger availability of nitrate in the electrolyte. As it will be shown later, indeed, the passivation of the lithium anode by the decomposition products of DOL results in the lower consumption of nitrate at the anode, making it available to react on the positive electrode. Once again, no feature attributable to oxygen reduction could be observed besides the higher initial OCP value. The Coulombic efficiency of the cell also decreases substantially, with approximately half the capacity being lost in the first charge. After 10 cycles, the capacity of the cell employing DME:DOL air is only 110 mAh g_s⁻¹ while the typical plateaus of sulfur are practically vanished.

Figure 2 shows the differential capacity plots of the discharge curves for the cells employing the various electrolytes. A characteristic that particularly stands out is the peak between 2.3 and 2.1 V vs. Li/Li⁺, corresponding to the sloping region in Figures 1a–1d. Such feature is much more evident when DME:DOL air is used as electrolyte. For DME:DOL Ar, in fact, only the first cycle shows a more prominent feature, rapidly decreasing for subsequent cycles. Similar results were shown in literature for solvents with a large concentration of the trisulfur radical anion,¹⁹ indicating that the amount of trisulfur radical might also be higher in the abovementioned cases.

As displayed in Figure 3, the pristine and cycled electrolytes were analyzed by ATR-IR. The dashed vertical lines mark two regions of interest for these electrolytes being solely associated to either DME or DOL. The bands around 1454 cm⁻¹ are due to the asymmetric deformation of the methyl group (-CH₃) in DME,²⁰ as confirmed by their absence in the spectrum of pure DOL too (labeled as ‘DOL electrolyte’ in Figure 3a). The band around 960 cm⁻¹ is, instead,

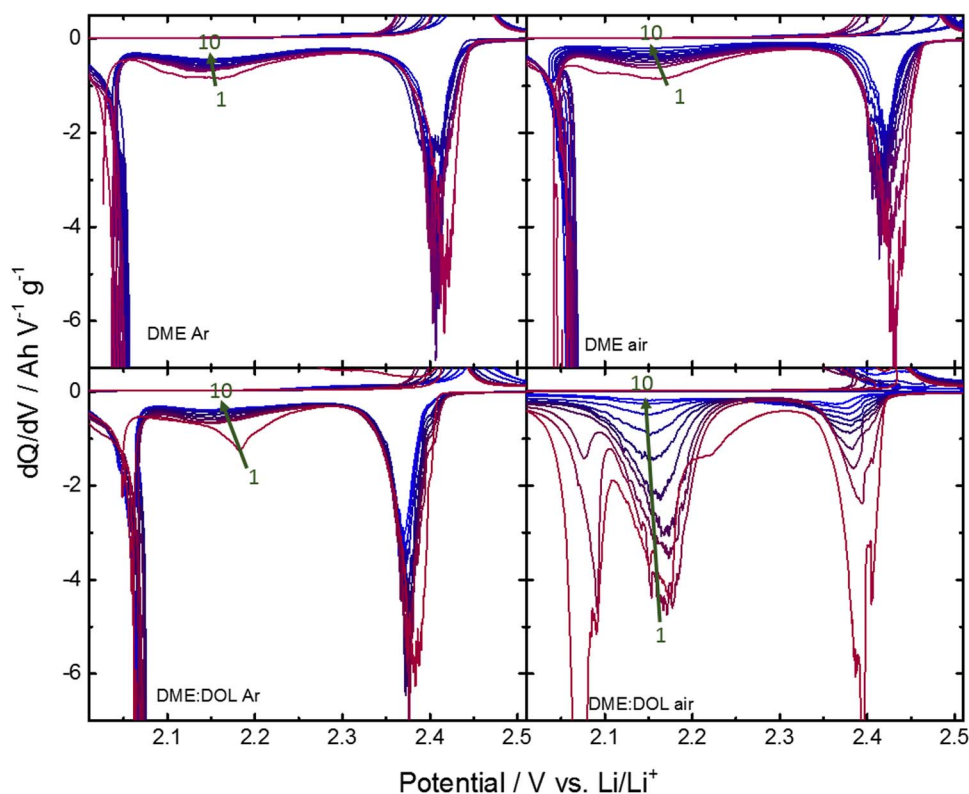


Figure 2. Differential capacity plots of the discharge curves (reported in Figure 1a–1d) of cells with a) DME Ar, b) DME air, c) DME:DOL Ar, and d) DME:DOL air electrolytes. The plots are focused in the region of major interest, i.e. between 2.0 and 2.5 V vs Li/Li⁺.

due to the ring stretching of DOL,²¹ and is therefore absent in the DME-based electrolyte.

From Figure 3, it is clear that DOL is consumed during cycling. The decrease of the DOL band upon cycling is stronger when oxygen is present, but it is also appreciated in the DME:DOL Ar electrolyte. Differently, the DME band is not strongly affected in any case. These findings are in agreement with those previously observed in Figure 1. Namely, oxygen has a stronger impact on DOL. The oxygen solubility in DME:DOL is similar to that in DME, calculated to be around 1.5 mmol L⁻¹ in both electrolytes,²² i.e., a higher amount of dissolved O₂ is not the reason for the increased decomposition. Thus, the decomposition mechanisms of DME and DOL must be different. As a matter of fact, it has been shown that DME reacts with oxygen superoxide to form esters, by bonding oxygen atoms to the carbon backbone of DME.¹⁷ By this mechanism, oxygen is consumed upon oxidation of DME, i.e., the decomposition will stop after all O₂ has reacted. Differently, being a cyclic compound, DOL is unsaturated and subject to ring opening reactions (ROR) leading to polymerization^{23,24} and isomerization.²⁵

Figure 4 depicts the proposed DOL decomposition mechanism in Li-S cells. Although we could not directly detect the presence of radicals, it is known from literature that they can start decomposition reactions of DOL,²⁵ so three sources of radicals are proposed: reduction of O₂ to form superoxide radical (when air is present), nitrate reduction products, and trisulfur radical anion (Figures 4a–4c, respectively). Of particular importance is the reduction of O₂, when present, in contact with metallic lithium, leading to the formation of lithium superoxide (Figure 4a). This species is known to be highly reactive, and, in fact, causes the increased DOL consumption when O₂ is present. From Figure 3, it is obvious that some DOL is consumed even in the absence of O₂, meaning that some other radical sources must be inherently present in the cell, forming radicals which are less reactive and/or in a smaller amount. For example, the electrolyte also contains LiNO₃ to aid the solid electrolyte interphase (SEI) formation on the lithium anode.^{10,26} The mechanism of nitrate reduction

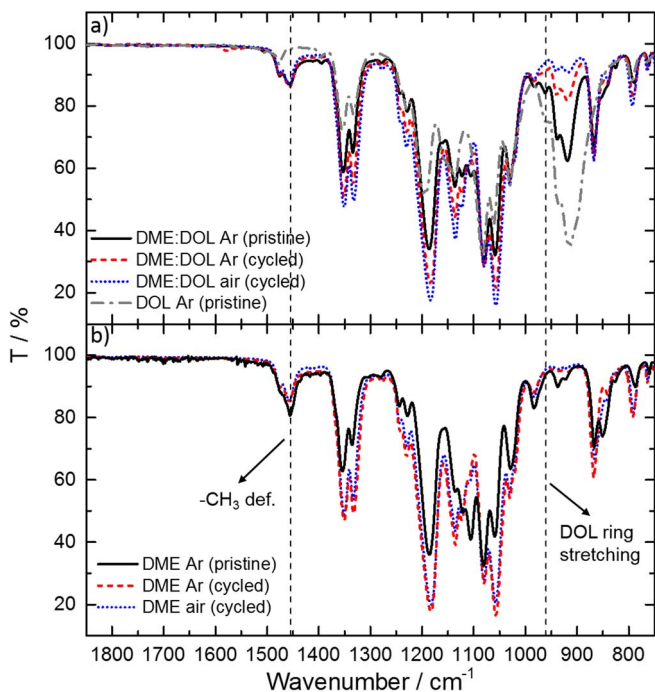


Figure 3. ATR-IR spectra of the different electrolytes: a) DME:DOL Ar (pristine), compared to DME:DOL Ar after 10 cycles (DME:DOL Ar (cycled)), DME:DOL air after 10 cycles (DME:DOL air (cycled)), and a solution of 1 mol L⁻¹ LiTFSI and 0.25 mol L⁻¹ LiNO₃ in DOL (DOL Ar); b) DME Ar (pristine), compared to DME Ar after 10 cycles (DME Ar (cycled)), and DME air after 10 cycles (DME air (cycled)).

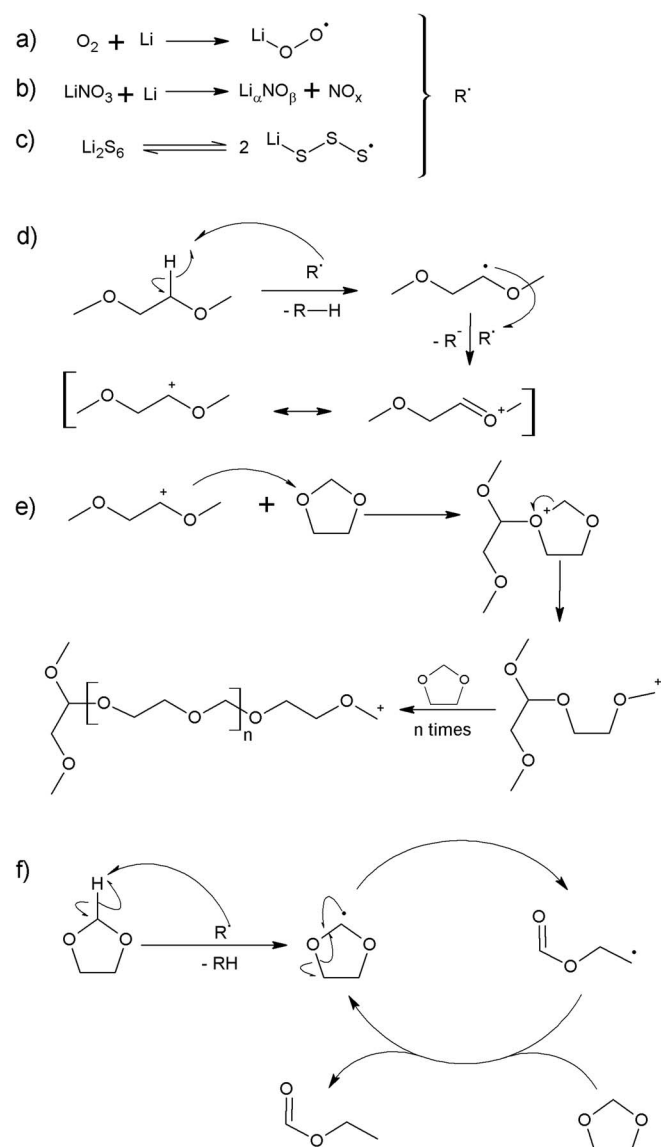


Figure 4. Proposed mechanisms of (a-c) radical formation in Li-S cells, (d-e) DOL polymerization, and (f) DOL isomerization.

in these electrolytes has not been fully elucidated yet, as studies on the subject often show only the decomposition products of $LiNO_3$ over the lithium surface.¹⁰ However, there has been some studies on nitrate reduction in molten-salt electrolytes²⁷ where the reduction occurs through the formation of lower nitrogen oxides and alkali metal oxides. Since ether-based electrolytes are aprotic, it is expected that the reduction of $LiNO_3$ follows a mechanism close to that occurring in molten salts (Figure 4b). Lastly, the presence of LiS_3^\bullet is inherent of Li-S cells^{12,19} (Figure 4c), and this radical could also react with the solvent.

Given the presence of radicals granted, the first mechanism for DOL decomposition is its polymerization, as shown in Figures 4d and 4e. It has been shown that DOL polymerization occurs neither through anionic²⁴ nor radical initiators,²⁵ but only via cationic polymerization. Thus, we propose a mechanism where the radicals in solution react with DME to form a carbocation (Figure 4d), which then reacts with DOL to start the polymerization (Figure 4e). Additionally, there might be other Lewis acids in solution, which could help initiating the polymerization as well. Polymerization of DOL has been already shown in Li- O_2 batteries, i.e., where molecular oxygen is present and dissolved in the electrolyte,^{17,28} as well as LSB.²⁶ Aurbach and coworkers²⁸

showed, for instance, that a silver electrode swept from 3.0 to 1.7 V vs Li/Li^+ in a 0.5 mol L^{-1} solution of $LiClO_4$ in DOL do not show any polymerization product over its surface. For the same system with added O_2 , some polyether species are detected on the silver surface by FTIR, showing that the products of O_2 reduction can indeed promote DOL polymerization, although the specific mechanism of polymerization in this setup was not determined. A similar phenomenon was reported by Bruce and coworkers¹⁷ in 1 mol L^{-1} $LiPF_6$ in DOL under 1 atm O_2 , although the excess of oxygen lead to further oxidation of polyether to form polyesters. In another work by Aurbach and coworkers,²⁹ lithium metal was exposed to pure DOL and DOL-based electrolytes (without oxygen). FTIR and XPS measurements of the surface of lithium showed hints for DOL decomposition, among which some peaks related to C-O bonds that the authors attributed to both polyether and alkoxide species. This is agreement with our findings reported in Figure 3a, in which DOL is consumed even when the electrolyte has no oxygen dissolved. Overall, all these previous reports are also in accordance with Figures 4a and 4b, where we show that DOL decomposition starts on the anode side. Interestingly, the last work by Aurbach et al.²⁹ also showed the presence of formate on the surface of lithium, which supports the reaction mechanism in Figure 4f, where direct reaction of DOL with radical species does not involve polymerization, but rather its isomerization to form ethyl formate.²⁵ This reaction is explained by the formation of a (strong) C=O bond, and takes place in parallel to the polymerization.

The formation of a polymeric film over the anode has a potentially good impact on the cell cycle life, since it avoids the reaction of polysulfides with metallic lithium. In fact, this might be one of the reasons for the early reports on DOL-containing electrolytes offering better performance,^{3,30,31} as those did not use SEI forming additives (e.g., $LiNO_3$).³² The presence of ethyl formate appears to be, however, very detrimental to the cell cycling life, since polysulfides can react with esters,^{4,18} forming electrochemically inert products.

According to the above-mentioned processes, Figure 5 shows the proposed mechanism which could explain the higher capacity observed in the sloping region (Figures 1 and 2). Ordinarily, only the reduction of S_8^{2-} to form S_4^{2-} is expected to happen extensively in this region. In fact, the S_8^{2-} disproportionation to form S_6^{2-} ($S_3^{\bullet-}$) and solid S_8 , was shown to be slow.¹⁹ The results shown in Figure 2 suggest, however, that S_8^{2-} reacts to form a (poly-thio)ester in the presence of an ester. This (poly-thio)ester is then reduced, forming the stable trisulfur radical anion and a thiocarboxylic radical, which is also stabilized by resonance. These two products are further reduced in the same voltage range resulting in the increased capacities observed in Figure 2. Interestingly, the IR spectra of the electrolytes after cycling (Figure 3) do not show peaks assignable to the carbonyl group. This suggests that the formed products are not present in solution. Since the products are not dissolved in the electrolyte, it follows that they must be insoluble in the ether-based electrolytes and are deposited on the electrodes. In order to support this hypothesis, EIS measurements were performed.

Figure 6a shows the Nyquist plots of AC/S cathodes (charged state) recorded during the initial 10 cycles in the various electrolytes while Figure 6b shows their magnification of the high-frequency region. The impedance spectra of the charged AC/S electrodes in DME Ar, DME air, and DME:DOL Ar, are very similar. They all show a depressed semi-circle in the high-frequency region (see magnifications in Figure 6b) followed by a capacitive- and diffusion-related feature in the mid- and low-frequency regions. The impedance spectra of AC/S electrode in DME:DOL air, however, are remarkably different, showing a much larger high-frequency semi-circle as well as the appearance of a second semicircle. Both features rapidly grow upon cycling. Overall, the impedance spectra resemble the trend seen in Figure 1, in that the electrochemical behavior of the AC/S electrode in the DME:DOL air electrolytes is rather different than in the other electrolytes (which are rather comparable to each other).

The high-frequency semi-circle is obviously associated to the electrode-electrolyte interface, being depressed by the porous electrode morphology and, possibly, the presence of a passive layer.³³

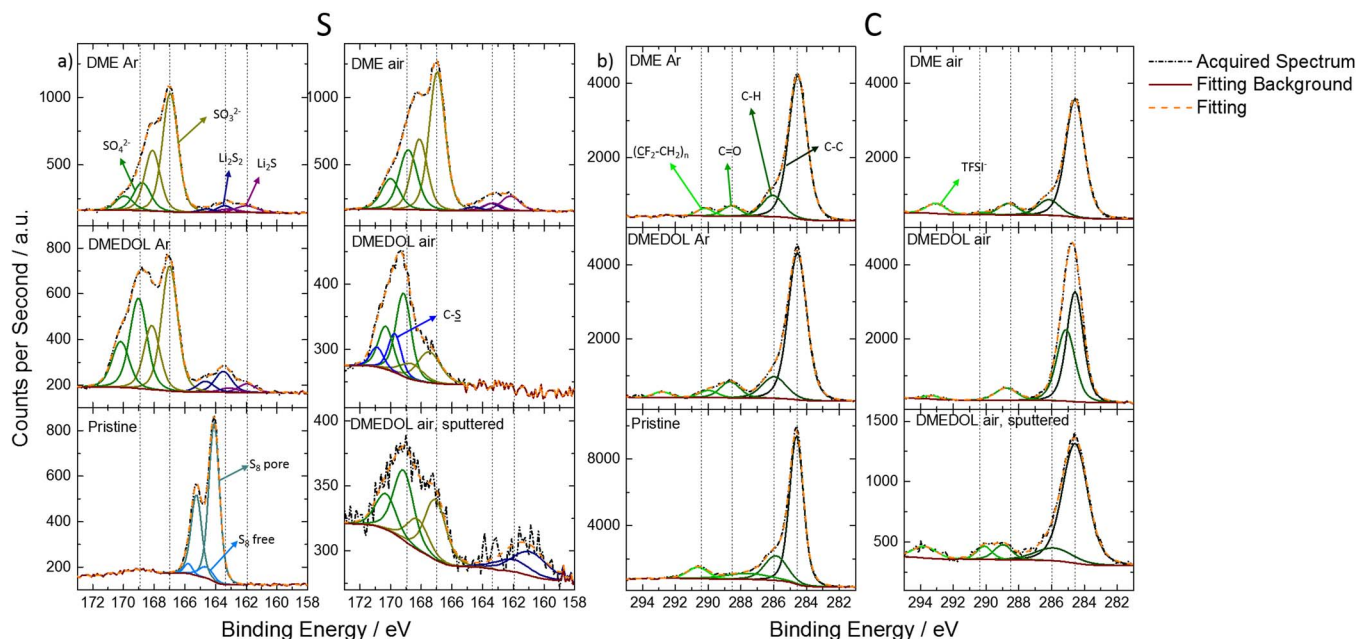


Figure 7. XPS spectra of a) sulfur, and b) carbon for charged AC/S electrodes (3.0 V vs Li/Li⁺) after cycling in the various electrolytes. The XPS spectra of the pristine electrodes are also shown for comparison. The cathode exposed to DME:DOL air was also sputtered for 2 minutes to remove the top layer. Black lines: raw data, brown lines: background, orange dashed lines: spectral envelopes.

As a matter of fact, this high-frequency feature is seen to increase upon cycling as the result of the passive layer growth. The rather larger diameter of this feature observed for the electrode in DME:DOL air already at the end of the 1st cycle, is clearly indicative of a thicker passive layer and, consequently, pore-clogging. Upon further cycling in this electrolyte, however, another depressed semi-circle appears in the mid-frequency range, which rapidly increases upon further cycling. The rapid evolution of both features may be associated with the reduction of sulfur in DME:DOL air leading to the formation of solid thio-carboxylates (see Figure 5), which are insoluble and precipitate initially at the electrode/electrolyte interface inside the porous electrode (pore clogging) and final over the electrode itself, causing the appearance of the second semi-circle. Such a rapid increase of the electrode impedance matches very well with the fast fading observed in Figure 1.

The evolution of the Li electrode impedance (Figures S4 and S5) confirms as the reactions of DOL start at the anode side, as the results suggest formation of a thick film over the lithium metal even before the cell started cycling, which is in accordance with the mechanism in Figures 4a, 4b, and 4c. The formed ester, however, dissolves into the electrolyte and migrates to the cathode where it reacts with the polysulfides forming solid deposits onto the AC/S cathode, thus explaining the rapid impedance increase upon cycling.

The AC/S cathodes were analyzed by SEM to check for morphological differences evolving upon cycling. As shown in Figure S6, while the activated carbon particles present in the pristine electrodes are still observable in the cathodes cycled in DME Ar, DME air, and DME:DOL Ar, the electrode operated in DME:DOL air is clearly different, showing a thick deposit of undefined morphology, and no distinguishable AC particles. This corroborates the EIS results reported in Figure 6, showing the growth of a thick passivation layer over the electrode.

Figure 7 shows the XPS spectra of the pristine and cycled (charged state) AC/S cathodes. The sulfur spectrum of the pristine cathode consists mostly of sulfur trapped inside AC pores (S 2p_{3/2} 164.1 eV)³³ and some small amount of free sulfur (S 2p_{3/2} 164.6 eV).³⁴ The carbon spectrum of the pristine electrode displays peaks for C-C bonds (C 1s 284.6 eV), C-H (C 1s 285.9 eV), C=O (C 1s 288.7 eV), and C-F (C 1s 290.5 eV), coming from AC and the PVdF binder.^{33,35,36}

The cathodes cycled in DME Ar, DME air, and DME:DOL Ar, present rather similar XPS peaks, although with varying intensities. The sulfur spectra show small peaks coming from Li₂S (S 2p_{3/2} 161.9 eV) and Li₂S₂ (S 2p_{3/2} 163.4 eV),³³ indicating some irreversibility upon charge, and more intense peaks from SO₃²⁻ (S 2p_{3/2} 166.9 eV) and SO₄²⁻ (S 2p_{3/2} 168.9 eV),³⁷ due to reactions with nitrate in the electrolyte.^{29,38} There is no visible sign of neutral sulfur, indicating that sulfur is not fully oxidized back to S₈. The XPS peaks of C were the same as observed in the pristine cathode, with the caveat that the C=O peak was sharper, suggesting some reaction between C and the nitrate. In some of the spectra, a small amount of TFSI⁻ is detected as well (C 1s 293.1 eV).³⁵ However, most importantly, the spectrum of the electrode cycled in DME:DOL air shows some striking differences. First, in the sulfur spectrum, no peaks associated to Li₂S or Li₂S₂ are observable, but only those related to SO₃²⁻ and SO₄²⁻. Another peak is also present, which is attributed to C-S bonds (S 2p_{3/2} 169.7 eV).³⁹ On the carbon side, there is no peak related to the binder's C-F bond. The peak related to C-H is much more intense and slightly shifted to lower binding energies, and the peak attributed to C=O is still present. The electrode was then subjected to sputtering in order to remove the top layer shown in the SEM image (Figure S6). As a result, the sulfur and carbon XPS spectra show the same general features as the other cathodes, e.g., the C-F peak of the binder becomes visible again. This is a substantial proof that the spectrum of the unsputtered electrode contains only peaks related to the passivation layer. The more intense C-H peak, then, is to be associated with the deposition of the alkoxides formed by the ester decomposition (see mechanism in Figure 4), which also explains the binding energy shift. Analogously, the C=O peak is due to the thiocarboxylate rather than oxidized AC, since the latter is covered by the passivation layer. This is also evidenced by the presence of a C-S peak in the sulfur spectrum. The appearance of formate and alkoxides is also in agreement with previous results in DOL-based electrolytes,^{17,29} further reinforcing the mechanisms proposed here.

Conclusions

In summary, the effect of dissolved O₂ (from dry air) in the state-of-the-art electrolyte for Li-S batteries (1 M LiTFSI, 0.25 M LiNO₃ in

DOL:DME) was investigated. It was observed that O₂ has a negative impact on the cells. Through *post mortem* analysis, it was possible to determine the products of electrolyte decomposition, and, in turn, indirectly determine the mechanism of decomposition. It was also shown how the proposed reactions affect the sulfur electrochemistry, and lead to increased capacity fading, which further strengthening the proposed mechanism.

Briefly, linear solvents, such as DME, are more resistant to decomposition by oxygen species, while DOL undergoes catalytic ring-opening reactions leading to fast solvent depletion. The cyclability of sulfur is affected by this decomposition of DOL (which starts at the anode side, before the cell is cycled). One proposed path of decomposition is radical-catalyzed isomerization of DOL, leading to the formation of esters, which react with the polysulfides. Such reaction increases the formation of trisulfur radical anion, electrochemically detected as the increased capacity of the sloping region during discharge. While this reaction eventually consumes all available active material, it also increases the capacity during the first discharge compared to ordinary electrolytes. This could also be determined by XPS of the cycled cathodes, which showed presence of thycarboxylate species.

Finally, DOL was shown to aid in the SEI formation in cells containing LiNO₃ as additive. DOL polymerizes on the anode, forming a more stable SEI than the one formed by only nitrate, as determined by EIS. Still, cells with and without DOL in the electrolyte provided similar specific capacity and capacity retention upon cycling. This suggests that, at least for the limited number of cycles investigated here, the presence of DOL is not imperative to obtain good capacity retention.

These results are especially important when investigating new additives to use in Li-S, for example, since, as is the case for LiNO₃, they could generate radicals in the electrolyte. These findings are also relevant to the field of Li-O₂ batteries, where these ether-based electrolytes are also used.

Acknowledgments

The authors thank Prof. Dr. Rolf Jürgen Behm and Dr. Thomas Diemant for performing XPS measurements. LL acknowledge the financial support from CNPq/Science without Borders program.

References

- D. A. Boyd, "Schwefel in Der Modernen Materialwissenschaft," *Angew. Chemie*, **2** (2016).
- D. Bresser, S. Passerini, and B. Scrosati, "Recent Progress and Remaining Challenges in Sulfur-Based Lithium Secondary Batteries – a Review," *Chem. Commun.*, **49**(90), 10545 (2013).
- J. Gao, M. A. Lowe, Y. Kiya, and H. D. Abruña, "Effects of Liquid Electrolytes on the Charge-Discharge Performance of Rechargeable Lithium/sulfur Batteries: Electrochemical and in-Situ X-Ray Absorption Spectroscopic Studies," *J. Phys. Chem. C*, **115**(50), 25132 (2011).
- T. Yim, Park, M.-S. Yu, J.-S. Kim, K. J. Im, K. Y. Kim, J.-H. Jeong, G. Jo, Y. N. Woo, S.-G. Kang, K. S. al., and "Effect of Chemical Reactivity of Polysulfide toward Carbonate-Based Electrolyte on the Electrochemical Performance of Li-S Batteries," *Electrochim. Acta*, **107**, 454 (2013).
- Y. X. Yin, S. Xin, Y. G. Guo, and L. J. Wan, "Lithium-Sulfur Batteries: Electrochemistry, Materials, and Prospects," *Angew. Chemie - Int. Ed.*, **52**(50), 13186 (2013).
- S. S. Zhang, "Liquid Electrolyte Lithium/sulfur Battery: Fundamental Chemistry, Problems, and Solutions," *J. Power Sources*, **231**, 153 (2013).
- Y. Diao, K. Xie, S. Xiong, and X. Hong, "Shuttle Phenomenon-The Irreversible Oxidation Mechanism of Sulfur Active Material in Li-S Battery," *J. Power Sources*, **235**, 181 (2013).
- Z. Lin, Z. Liu, W. Fu, N. J. Dudney, and C. Liang, "Phosphorous Pentasulfide as a Novel Additive for High-Performance Lithium-Sulfur Batteries," *Adv. Funct. Mater.*, **23**(8), 1064 (2013).
- F. Wu, J. T. Lee, N. Nitta, H. Kim, O. Borodin, and G. Yushin, "Lithium Iodide as a Promising Electrolyte Additive for Lithium-Sulfur Batteries: Mechanisms of Performance Enhancement," *Adv. Mater.*, **27**(1), 101 (2015).
- X. Liang, Z. Wen, Y. Liu, M. Wu, J. Jin, H. Zhang, and X. Wu, "Improved Cycling Performances of Lithium Sulfur Batteries with LiNO₃-Modified Electrolyte," *J. Power Sources*, **196**(22), 9839 (2011).
- B. D. McCloskey, D. S. Bethune, R. M. Shelby, G. Girishkumar, and A. C. Luntz, "Solvents' Critical Role in Nonaqueous Lithium-Oxygen Battery Electrochemistry," *J. Phys. Chem. Lett.*, **2**(10), 1161 (2011).
- Q. Wang, Zheng, J. Walter, E. Pan, H. Lv, D. Zuo, P. Chen, H. Deng, Z. D. Liaw, B. Y. Yu, X. al., and "Direct Observation of Sulfur Radicals as Reaction Media in Lithium Sulfur Batteries," *J. Electrochem. Soc.*, **162**(3), A474 (2015).
- M. Cuisinier, P. E. Cabelguen, S. Evers, G. He, M. Kolbeck, A. Garsuch, T. Bolin, M. Balasubramanian, and L. F. Nazar, "Sulfur Speciation in Li-S Batteries Determined by Operando X-Ray Absorption Spectroscopy," *J. Phys. Chem. Lett.*, **4**(19), 3227 (2013).
- S. S. Zhang, "Effect of Discharge Cutoff Voltage on Reversibility of Lithium/Sulfur Batteries with LiNO₃-Contained Electrolyte," *J. Electrochem. Soc.*, **159**(7), A920 (2012).
- J. Christensen, P. Albertus, R. S. Sanchez-Carrera, T. Lohmann, B. Kozinsky, R. Liedtke, J. Ahmed, and A. Kojic, "A Critical Review of Li/Air Batteries," *J. Electrochem. Soc.*, **159**(2), R1 (2012).
- N. Imanishi and O. Yamamoto, "Rechargeable Lithium-Air Batteries: Characteristics and Prospects," *Mater. Today*, **17**(1), 24 (2014).
- S. A. Freunberger, Y. Chen, N. E. Drewett, L. J. Hardwick, F. Bardé, and P. G. Bruce, "The Lithium-Oxygen Battery with Ether-Based Electrolytes," *Angew. Chemie Int. Ed.*, **50**(37), 8609 (2011).
- Mc Murry, J. Ester Cleavages via S N 2-Type Dealkylation. In *Organic Reactions*, John Wiley & Sons, Inc.: Hoboken, NJ, USA, 2011, Vol. 24, pp 187.
- M. Cuisinier, C. Hart, M. Balasubramanian, A. Garsuch, and L. F. Nazar, "Radical or Not Radical: Revisiting Lithium-Sulfur Electrochemistry in Nonaqueous Electrolytes," *Adv. Energy Mater.*, **5**(16), 1 (2015).
- H. Yoshida and H. Matsuura, "Density Functional Study of the Conformations and Vibrations of 1, 2-Dimethoxyethane," *J. Phys. Chem. A*, **102**(16), 2691 (1998).
- J. Makarewicz and T. Ha, "Ab Initio Study of the Pseudorotation in 1,3-Dioxolane," *J. Mol. Struct.*, **599**(1-3), 271 (2001).
- J. Read, "Characterization of the Lithium/Oxygen Organic Electrolyte Battery," *J. Electrochem. Soc.*, **149**(9), A1190 (2002).
- Y. L. Berman, Y. B. Lyudvig, V. A. Ponomarenko, and S. S. Medvedev, "Mechanism of the Polymerization of 1,3-Dioxolane," *Polym. Sci. U.S.S.R.*, **11**(1), 225 (1969).
- M. Okada, Y. Yamashita, and Y. Ishii, "Polymerization of 1,3-Dioxolane," *Makromolekulare*, (1964), 196.
- W. J. Bailey, "Free Radical Ring-Opening Polymerization," *Die Makromol. Chemie*, **13**(S19851), 171 (1985).
- D. Aurbach, E. Pollak, R. Elazari, G. Salitra, C. S. Kelley, and J. Affinito, "On the Surface Chemical Aspects of Very High Energy Density, Rechargeable Li-Sulfur Batteries," *J. Electrochem. Soc.*, **156**(8), A694 (2009).
- P. G. Zamboni, "Oxide Chemistry and Electroreduction of NO₃⁻ in Molten Alkali Nitrates," *J. Electroanal. Chem. Interfacial Electrochem.*, **24**(2-3), 365 (1970).
- D. Aurbach, O. Youngman, and P. Dan, "The Electrochemical Behavior of 1,3-dioxolane—LiClO₄ solutions—II. Contaminated Solutions," *Electrochim. Acta*, **35**(3), 639 (1990).
- D. Aurbach, E. Pollak, R. Elazari, G. Salitra, C. S. Kelley, and J. Affinito, "On the Surface Chemical Aspects of Very High Energy Density, Rechargeable Li-Sulfur Batteries," *J. Electrochem. Soc.*, **156**(8), A694 (2009).
- D. R. Chang, S. H. Lee, S. W. Kim, and H. T. Kim, "Binary Electrolyte Based on Tetra(ethylene Glycol) Dimethyl Ether and 1,3-Dioxolane for Lithium-Sulfur Battery," *J. Power Sources*, **112**(2), 452 (2002).
- W. Wang, Y. Wang, Y. Huang, C. Huang, Z. Yu, H. Zhang, A. Wang, and K. Yuan, "The Electrochemical-Performance of Lithium-Sulfur Batteries with LiClO₄ DOL/DME Electrolyte," *J. Appl. Electrochem.*, **40**(2), 321 (2010).
- S. S. Zhang, "Role of LiNO₃ in Rechargeable Lithium/sulfur Battery," *Electrochim. Acta*, **70**, 344 (2012).
- M. Helen, M. A. Reddy, T. Diemant, U. Golla-Schindler, R. J. Behm, U. Kaiser, and M. Fichtner, "Single Step Transformation of Sulphur to Li₂S₂/Li₂S in Li-S Batteries," *Sci. Rep.*, **5**, 12146 (2015).
- A. S. Manocha and R. L. Park, "Flotation Related ESCA Studies on PbS Surfaces," *Appl. Surf. Sci.*, **1**(1), 129 (1977).
- B. Sun, C. Xu, J. Mindemark, T. Gustafsson, K. Edström, and D. Brandell, "At the Polymer Electrolyte Interfaces: The Role of the Polymer Host in Interphase Layer Formation in Li-Batteries," *J. Mater. Chem. A*, **3**(26), 13994 (2015).
- D. T. Clark, W. J. Feast, D. Kilcast, and W. K. R. Musgrave, "Applications of ESCA to Polymer Chemistry. III. Structures and Bonding in Homopolymers of Ethylene and the Fluoroethylenes and Determination of the Compositions of Fluoro Copolymers," *J. Polym. Sci. Polym. Chem. Ed.*, **11**(2), 389 (1973).
- R. V. Siritwardane and J. M. Cook, "Interactions of SO₂ with Sodium Deposited on CaO," *J. Colloid Interface Sci.*, **114**(2), 525 (1986).
- Y. Diao, K. Xie, S. Xiong, and X. Hong, "Insights into Li-S Battery Cathode Capacity Fading Mechanisms: Irreversible Oxidation of Active Mass during Cycling," *J. Electrochem. Soc.*, **159**(11), A1816 (2012).
- T. X. Carroll, D. Ji, D. C. Maclaren, T. D. Thomas, and L. J. Saethre, "Relativistic Corrections to Reported Sulfur 1s Ionization Energies," *J. Electron Spectros. Relat. Phenomena*, **42**(3), 281 (1987).
- L. Bai and B. E. Conway, "AC Impedance of faradaic Reactions Involving Electrodesorbed Intermediates: Examination of Conditions Leading to Pseudoinductive Behavior Represented in Three-Dimensional Impedance Spectroscopy Diagrams," *J. Electrochem. Soc.*, **138**(10), 2897 (1991).